

This discussion paper is/has been under review for the journal Atmospheric Measurement Techniques (AMT). Please refer to the corresponding final paper in AMT if available.

# High-accuracy continuous airborne measurements of greenhouse gases (CO<sub>2</sub> and CH<sub>4</sub>) during BARCA

H. Chen<sup>1</sup>, J. Winderlich<sup>1</sup>, C. Gerbig<sup>1</sup>, A. Hofer<sup>1</sup>, C. W. Rella<sup>2</sup>, E. R. Crosson<sup>2</sup>,  
A. D. Van Pelt<sup>2</sup>, J. Steinbach<sup>1</sup>, O. Kolle<sup>1</sup>, V. Beck<sup>1</sup>, B. C. Daube<sup>3</sup>, E. W. Gottlieb<sup>3</sup>,  
V. Y. Chow<sup>3</sup>, G. W. Santoni<sup>3</sup>, and S. C. Wofsy<sup>3</sup>

<sup>1</sup>Max Planck Institute for Biogeochemistry, 07745 Jena, Germany

<sup>2</sup>Picarro, Inc., Sunnyvale, CA 94085, USA

<sup>3</sup>Department of Earth and Planetary Sciences and the Division of Engineering and Applied Sciences, Harvard University, Cambridge, Massachusetts, USA

Received: 19 November 2009 – Accepted: 25 November 2009 – Published: 4 December 2009

Correspondence to: H. Chen (hchen@bgc-jena.mpg.de)

Published by Copernicus Publications on behalf of the European Geosciences Union.

**High-accuracy  
continuous airborne  
measurements of  
greenhouse gases**

H. Chen et al.

Title Page

Abstract

Introduction

Conclusions

References

Tables

Figures

◀

▶

◀

▶

Back

Close

Full Screen / Esc

Printer-friendly Version

Interactive Discussion

## Abstract

High-accuracy continuous measurements of greenhouse gases (CO<sub>2</sub> and CH<sub>4</sub>) during the BARCA (Balanço Atmosférico Regional de Carbono na Amazônia) phase B campaign in Brazil in May 2009 were accomplished using a newly available analyzer based on the cavity ring-down spectroscopy (CRDS) technique. This analyzer was flown without a drying system or any in-flight calibration gases. Water vapor corrections associated with dilution and pressure-broadening effects for CO<sub>2</sub> and CH<sub>4</sub> were derived from laboratory experiments employing measurements of water vapor by the CRDS analyzer. Before the campaign, the stability of the analyzer was assessed by laboratory tests under simulated flight conditions. During the campaign, a comparison of CO<sub>2</sub> measurements between the CRDS analyzer and a nondispersive infrared (NDIR) analyzer on board the same aircraft showed a mean difference of 0.22±0.09 ppm for all flights over the Amazon rain forest. At the end of the campaign, CO<sub>2</sub> concentrations of the synthetic calibration gases used by the NDIR analyzer were determined by the CRDS analyzer. After correcting for the isotope and the pressure-broadening effects that resulted from changes of the composition of synthetic vs. ambient air, and applying those concentrations as calibrated values of the calibration gases to reprocess the CO<sub>2</sub> measurements made by the NDIR, the mean difference between the CRDS and the NDIR during BARCA was reduced to 0.05±0.09 ppm, with the mean standard deviation of 0.23±0.05 ppm. The results clearly show that the CRDS is sufficiently stable to be used in flight without drying the air or calibrating in flight and the water corrections are fully adequate for high-accuracy continuous airborne measurements of CO<sub>2</sub> and CH<sub>4</sub>.

## 1 Introduction

Efforts to measure the concentration of carbon dioxide (CO<sub>2</sub>) in the atmosphere to obtain the temporal and geographic distribution of atmospheric CO<sub>2</sub> have been made

AMTD

2, 3127–3152, 2009

### High-accuracy continuous airborne measurements of greenhouse gases

H. Chen et al.

Title Page

Abstract

Introduction

Conclusions

References

Tables

Figures

⏪

⏩

◀

▶

Back

Close

Full Screen / Esc

Printer-friendly Version

Interactive Discussion

**High-accuracy  
continuous airborne  
measurements of  
greenhouse gases**

H. Chen et al.

Title Page

Abstract

Introduction

Conclusions

References

Tables

Figures

⏪

⏩

◀

▶

Back

Close

Full Screen / Esc

Printer-friendly Version

Interactive Discussion

since the 1930s. Measurements of CO<sub>2</sub> play an important role in understanding the global carbon cycle and its contribution to the global warming (Bischof, 1962; Keeling et al., 1968; Tans et al., 1996; Heimann, 2009). In recent years, methane (CH<sub>4</sub>) has received increasing attention as the second most important greenhouse gas after CO<sub>2</sub> because of the high uncertainty of its sinks and sources (Houweling et al., 2006; Kessler et al., 2006; Miller et al., 2007; Frankenberg et al., 2008). Among the wide variety of platforms (from ground-based stations, towers, ships, aircraft and balloons to satellites) on which CO<sub>2</sub> and CH<sub>4</sub> measurements can be acquired, aircraft measurements are essential for observations in the free troposphere and lower stratosphere covering regional to continental scales. However, obtaining measurements on board aircraft is challenging due to the difficulty of ensuring high accuracy under severe conditions of changing pressure and temperature as well as mechanical stress due to shock and vibration. Therefore, initially the primary method of acquiring airborne CO<sub>2</sub> and CH<sub>4</sub> measurements was to collect air samples in flasks or other containers during a flight and analyze the air later in the laboratory (Keeling et al., 1968). Even nowadays, flask measurements are still a reliable way for airborne measurements to determine concentrations of species of interest in the atmosphere. Although very reliable, flask measurements have limitations which restrict its ability to capture temporal and spatial variability information, especially for observations within the boundary layer. During the last 30 years, high-accuracy in situ airborne CO<sub>2</sub> measurements (mainly using the NDIR technique) have been carried out both in aircraft campaigns and in routine flights (Boering et al., 1994; Anderson et al., 1996; Daube et al., 2002; Machida et al., 2002; Shashkov et al., 2007; Machida et al., 2008). However, only in recent years has high-accuracy in situ CH<sub>4</sub> instrumentation become available for airborne measurements (Jimenez et al., 2005).

In this paper, we present a high-accuracy analyzer using the wavelength-scanned cavity ring-down spectroscopy (CRDS) technique for continuous measurements of CO<sub>2</sub> and CH<sub>4</sub> with minimum maintenance in the field during the BARCA phase B campaign in Brazil in May 2009. Unlike all previous techniques, this analyzer is able to monitor

---

**High-accuracy  
continuous airborne  
measurements of  
greenhouse gases**H. Chen et al.

---

[Title Page](#)[Abstract](#)[Introduction](#)[Conclusions](#)[References](#)[Tables](#)[Figures](#)[⏪](#)[⏩](#)[◀](#)[▶](#)[Back](#)[Close](#)[Full Screen / Esc](#)[Printer-friendly Version](#)[Interactive Discussion](#)

atmospheric CO<sub>2</sub> and CH<sub>4</sub> highly accurately without the need to dry the sample air or to employ in-flight calibrations. It was necessary to perform in-flight calibrations and careful air drying techniques in all in situ airborne measurements of CO<sub>2</sub> and CH<sub>4</sub> within the troposphere in order to guarantee measurement accuracy. The need for calibration was driven by the lack of stability of the analyzers within a flight period under changing pressure and temperature conditions, while the reason for drying the air was the difficulty of measuring water vapor precisely. The high performance and low maintenance of the CRDS analyzer has made it the choice as the analyzer for measurements of greenhouse gases on board a commercial airliner within a European Union project of In-service Aircraft for a Global Observing System (IAGOS).

This paper describes techniques and presents results of laboratory experiments necessary to validate and verify CRDS analyzer performance before deployment. The measurement principle used in this analyzer is introduced in Sect. 2. Then the laboratory experiments used to derive the water correction functions for CO<sub>2</sub> and CH<sub>4</sub> and to assess the performance under simulated flight conditions are described in Sects. 3 and 4, respectively. In Sect. 5 we compare airborne CO<sub>2</sub> measurements of the CRDS analyzer with independent measurements made by an NDIR analyzer. Section 6 discusses a cross-calibration for the two analyzers and Sect. 7 concludes the paper.

## 2 The CRDS analyzer

CRDS is a technique which introduces a gas sample into a high-finesse optical cavity; subsequently, the optical absorbance of the sample is determined by the light dissipation rate in the optical cavity, thus providing parts-per-billion concentration or isotopic ratio measurements of a particular gas species of interest which is unaffected by the initial strength of the light source. This technique has been successfully implemented in a ground-based greenhouse gas analyzer (Crosson, 2008). The analyzer employs two lasers, a high-precision wavelength monitor, a high finesse optical cavity with three high-reflectivity mirrors (>99.995%) and a photodetector. During the measurements,

**High-accuracy  
continuous airborne  
measurements of  
greenhouse gases**

H. Chen et al.

Title Page

Abstract

Introduction

Conclusions

References

Tables

Figures

⏪

⏩

◀

▶

Back

Close

Full Screen / Esc

Printer-friendly Version

Interactive Discussion

light at a specific wavelength from a laser is injected into the cavity through a partially reflecting mirror. The light intensity then builds up over time and is monitored through a second partially reflecting mirror using a photodetector located outside the cavity. The “ring-down” measurement is made by rapidly turning off the laser and measuring the time constant of the light intensity as it exponentially decays. The lasers are tuned to scan over the individual spectral lines of  $^{12}\text{C}^{16}\text{O}_2$ ,  $^{12}\text{CH}_4$  and  $\text{H}_2^{16}\text{O}$  producing a high resolution spectrum of each. Fits to each of these high-resolution absorption spectrum are then obtained, from which the constituent quantities of the gas sample is determined. The flight analyzer (Picarro Inc., CA, USA, model G1301-m) was developed on the basis of a previous model, G1301. Because the performance requirements of the flight analyzer and environmental conditions seen in flight are considerably more difficult to meet than are those for the standard G1301 product, significant modifications were undertaken which resulted in new hardware, electronics, and software. These changes included a) adding an ambient pressure sensor and applying an ambient pressure correction to the high-precision wavelength monitor to ensure wavelength targets are met correctly under quickly changing ambient pressure; b) introducing three additional temperature sensors strategically located on the CRDS cavity and new firmware to enable correct operation of the analyzer’s sample, pressure and temperature control systems; c) replacing the computer hard drive with solid state memory; d) increasing the data acquisition rate of the analyzer from 0.2 Hz to 0.5 Hz.

### 3 Laboratory experiments to derive water correction functions

Atmospheric water vapor varies over small temporal and spatial scales and thus influences the measured  $\text{CO}_2$  and  $\text{CH}_4$  by dilution and pressure-broadening effects. To avoid the influence due to the dilution effect,  $\text{CO}_2$  and  $\text{CH}_4$  mixing ratios are always reported as dry mole fractions. In order to ensure the measurement accuracy of  $\text{CO}_2$  better than 0.1 ppm for measurements in the southern hemisphere according to the WMO recommendation (WMO, 2003) at 400 ppm level, the water vapor in the sam-

ple air is either required to be removed to a level below 250 ppm or simultaneously measured at a precision of below 250 ppm to correct the water vapor dilution effect. Furthermore, spectral measurements are sensitive to water vapor through pressure broadening. Here we assess whether the water measurements are adequate for correcting the dilution and the pressure-broadening effects.

### 3.1 Experiments

In order to derive water correction functions for CO<sub>2</sub> and CH<sub>4</sub>, a series of experiments were carried out (see Fig. 1). Gas from an ambient air tank was supplied to a humidifier. After it was humidified, the gas was split into two paths, one with and the other without a chemical dryer (magnesium perchlorate). Carefully balancing the flow and pressure ensures that there was no change in pressure in the chemical dryer while switching. This avoided the influence of magnesium perchlorate under conditions of changing pressure on CO<sub>2</sub> mixing ratios (Levin et al., 2002). The crossover valve downstream of the dryer was controlled by a data logger that selected dry or wet air to flow through the CRDS analyzer.

The humidifier was sequentially set to dew points 0°C, 5°C, 10°C, 15°C, 20°C, 25°C, 30°C and 35°C, corresponding to reported water vapor mixing ratios from 0.6% to 6%. The experiments were performed in a temperature-controlled room (~38°C) to prevent water vapor from condensing on the walls of tubing before flowing into the CRDS analyzer. The experiments were interrupted several times when the chemical dryer had to be changed.

The CO<sub>2</sub> mixing ratio of the gas downstream of the humidifier often drifted linearly or exponentially due to the interaction between CO<sub>2</sub> and water in the humidifier. The drifts were removed before calculating the mixing ratio for both dry and wet cycles. The CH<sub>4</sub> mixing ratio was calculated in the same way as the CO<sub>2</sub> mixing ratio, however, the corrected drift was insignificant since no interaction between CH<sub>4</sub> and water occurred (see Fig. 2a,b). The precision of the measurement of the water vapor mixing ratio of the CRDS analyzer is 23 ppm (1σ) at reported 4% H<sub>2</sub>O level (the maximum

## High-accuracy continuous airborne measurements of greenhouse gases

H. Chen et al.

Title Page

Abstract

Introduction

Conclusions

References

Tables

Figures

⏪

⏩

◀

▶

Back

Close

Full Screen / Esc

Printer-friendly Version

Interactive Discussion



[Title Page](#)[Abstract](#)[Introduction](#)[Conclusions](#)[References](#)[Tables](#)[Figures](#)[⏪](#)[⏩](#)[◀](#)[▶](#)[Back](#)[Close](#)[Full Screen / Esc](#)[Printer-friendly Version](#)[Interactive Discussion](#)

H<sub>2</sub>O level during the campaign, excluding the cases of flying through cloud or rain), which is precise enough for correcting the dilution effect. In fact, both the dilution and the pressure-broadening effects can be compensated by the reported H<sub>2</sub>O mixing ratios. The effects of water vapor dilution as well as of pressure broadening for CO<sub>2</sub> and CH<sub>4</sub> can be represented by quadratic fits,  $CO_{2wet}/CO_{2dry}=1+a\times H_2O+b\times H_2O^2$  and  $CH_{4wet}/CH_{4dry}=1+c\times H_2O+d\times H_2O^2$ ,  $a=-0.012000$ ,  $b=-0.000267$ ,  $c=-0.009823$ ,  $d=-0.000239$  (see Fig. 2c,d). The residual errors of the fits were below 0.05 ppm for CO<sub>2</sub> and below 0.8 ppb for CH<sub>4</sub>.

### 3.2 Transferability of the water correction functions

It is important to assess if the coefficients of the water correction functions derived from the laboratory experiment can be regarded as constants or whether a recalibration of these parameters via laboratory experiment is required. Rather than repeating the experiments at different times, e.g. after a year, we decided to repeat the experiment with a different analyzer. The assumption is that if the coefficients are transferable between instruments, they are also likely to not change over time.

We compared water correction functions of the flight CRDS analyzer (model G1301-m, serial designation CFADS37) with those of one ground-based CRDS analyzer (model G1301, serial designation CFADS15). We use CFADS37 and CFADS15 throughout the subsequent text to differentiate the two CRDS analyzers.

Similar experiments were done with CFADS15; however, the applied water vapor mixing ratios ranged from 0.61% to 2.76%. To calibrate the water vapor measurement of CFADS15 against CFADS37, step-changing wet air (from 1.09% to 2.11%) from a humidifier was provided to the two analyzers simultaneously. The water vapor measurements of the two analyzers are linearly correlated. After the calibration of the water vapor measurement, the water vapor correction functions from the experiments for CFADS37 were applied to the experimental results of CFADS15 (see Fig. 2e,f). Comparable residual errors (below 0.05 ppm for CO<sub>2</sub> and below 0.5 ppb for CH<sub>4</sub>) ob-

tained from applying the same water correction functions to both experimental results for CFADS37 and CFADS15 proved that these correction functions are transferable from one instrument to another if the water vapor measurements are calibrated to the same scale.

5 Because the water vapor measurement by the analyzer is based on a single stable H<sub>2</sub>O spectroscopic feature which is spectrally close to the CH<sub>4</sub> spectral feature, we expect the measurement of the water vapor to exhibit the same highly stable performance over time that has been demonstrated on both CO<sub>2</sub> and CH<sub>4</sub>. Due to the difficulties in providing a known amount of water vapor, we cannot directly estimate the drift of water  
10 vapor accurately. However, we can use other stable gas measurements from the same analyzer (i.e. CO<sub>2</sub> and CH<sub>4</sub>) to estimate the drifts we might expect to see in H<sub>2</sub>O since the spectroscopy shares the same components (only the spectral lines are different). In CO<sub>2</sub>, these analyzers appear to drift less than 0.5 ppm (Richardson et al., 2009) over two years of operating time, which corresponds to a drift of 1 part in 800 of the  
15 400 ppm CO<sub>2</sub> concentration. That would indicate that a 4% water vapor concentration should drift by no more than 1 part in 800 of 4%, or 50 ppm. Drift of 50 ppm in the water vapor concentration translates to just drift of 0.02 ppm or 0.1 ppb in the final reported CO<sub>2</sub> and CH<sub>4</sub> mixing ratios, respectively.

#### 4 Performance under simulated flight conditions

20 A flight analyzer needs to be able to deal with the environmental temperature and pressure variations on board aircraft. As part of the work necessary to verify CRDS analyzer performance before deployment in the field, we applied temperature and pressure variations that typically occurred during flight. To this end we placed the CRDS analyzer in an environmental chamber in an attempt to replicate the conditions found  
25 aboard a research aircraft (Bandeirante EMB 110) with a non-pressurized cabin flying over the Amazon rain forest in Brazil or aboard a commercial airliner (Airbus A340). The analyzer measured a standard gas during the whole test period. The test results

Title Page

Abstract

Introduction

Conclusions

References

Tables

Figures

◀

▶

◀

▶

Back

Close

Full Screen / Esc

Printer-friendly Version

Interactive Discussion



are shown in Fig. 3. The instrument ambient pressure ranged from 1000 mbar down to 640 mbar and temperature ranged from 44°C down to 26°C covering the expected range of cabin conditions typically found on board both aircraft. Note that the instrument aboard the Airbus A340 usually experiences ambient pressure down to 250 mbar, which was not tested during this experiment; however the inlet pressure control system of the analyzer is designed to cover this range of inlet pressures.

The measurements during laboratory pressure and temperature tests indicate undisturbed stability and slightly larger noise under simulated flight conditions (400.59±0.09 ppm for CO<sub>2</sub> and 1950.07±0.68 ppb for CH<sub>4</sub>) compared to under normal ambient conditions (400.59±0.07 ppm for CO<sub>2</sub> and 1950.15±0.64 ppb for CH<sub>4</sub>). The maximum pressure change rate was actually 5 times larger than what was expected to happen aboard research aircraft or aboard commercial aircraft due to the operational constraints of the environmental chamber. The performance of the CRDS analyzer under simulated flight conditions implies high stability during later flight measurements.

## 5 In-flight Comparison of the CRDS with an NDIR analyzer

Besides the CRDS analyzer, an NDIR CO<sub>2</sub> analyzer (modified Li-Cor, Inc. LI-6251) was also flown on board the same aircraft during the entire campaign. A detailed description of this instrument is given in Daube et al. (2002); here we only describe the points that are related to the comparison of CO<sub>2</sub> measurements of the CRDS with the NDIR analyzer. The NDIR system employs a two-step drying system that is able to remove the water vapor in the sample air sufficiently and minimizes the effect on the instrument's response time. Four standard gases are used for in-flight NDIR CO<sub>2</sub> calibrations. The data from the NDIR analyzer were recorded at 4 Hz and were median-filtered within 2 s. The time delay between the time air enters the inlet until it reaches the sample cell varies according to the bypass flow and relevant volumes. As a result, a variable time delay correction was applied to the final data (Daube et al., 2002). The time delay during the BARCA phase B was between 3.2 s and 4.1 s.

[Title Page](#)[Abstract](#)[Introduction](#)[Conclusions](#)[References](#)[Tables](#)[Figures](#)[⏪](#)[⏩](#)[◀](#)[▶](#)[Back](#)[Close](#)[Full Screen / Esc](#)[Printer-friendly Version](#)[Interactive Discussion](#)

The CRDS analyzer measured the three species of CO<sub>2</sub>, CH<sub>4</sub> and H<sub>2</sub>O sequentially. CO<sub>2</sub> was measured every 1.5 s, while CH<sub>4</sub> and H<sub>2</sub>O were measured every 3.0 s. The timestamp of each measurement made by the CRDS analyzer corresponded to the completion of the spectral scan of each gas species, thus specifying the actual time when the sample was being measured to within a few hundred milliseconds. Laboratory tests showed that the sample flow rate (~460 sccm) of the CRDS analyzer was rather constant (less than 5% change) over the change of the ambient pressure from 330 mbar to 1330 mbar. The time delay was corrected based on the ambient pressure, the flow rate and estimated relevant volumes.

During the BARCA phase B campaign, 16 flights were made, including one test flight in Sao Jose dos Campos and 15 flights over the Amazon rain forest. Table 1 shows the comparisons of the measurements of the two CO<sub>2</sub> analyzers. The missing values in the table are due to missing data for one of the analyzers or, in the worst case, both. The CRDS analyzer did not operate for two of the flights due to the failure of one temperature controller inside the analyzer for flights nos. 008 and 009, while the NDIR analyzer did not operate due to the failure of a pump in the case of flights nos. 009 and 010 and was not operated in the case of flight no. 014 to avoid catching rainwater.

With the test flight data removed (flight no. 000), before which calibration gases had been sitting for almost half a year and during which the space inside the aircraft was severely overheated, the mean difference over all subsequent flights is 0.22±0.09 ppm, and the mean standard deviation of the difference is 0.23±0.05 ppm. The time differences between the measurements of the two analyzers obtained by maximizing the correlation of the measurements in each individual flight are -0.2±1.2 s, which is smaller than the time resolution of the CRDS analyzer (1.5 s) or of the reported NDIR results (2 s).

**High-accuracy  
continuous airborne  
measurements of  
greenhouse gases**

H. Chen et al.

Title Page

Abstract

Introduction

Conclusions

References

Tables

Figures

⏪

⏩

◀

▶

Back

Close

Full Screen / Esc

Printer-friendly Version

Interactive Discussion

## 6 Cross-calibration during the BARCA campaign

Four filling tanks were used to refill the internal small calibration cylinders in the NDIR analyzer during the campaign. Among the four filling tanks, three were calibrated at the Department of Earth and Planetary Sciences and the Division of Engineering and Applied Sciences at Harvard about one year prior to the campaign, and one reference gas tank was obtained in Brazil and calibrated by the flight NDIR analyzer in the field. All of the four tanks contained synthetic air.

The CRDS analyzer was calibrated using four ambient air standards in the laboratory of Max Planck Institute for Biogeochemistry (MPI) in Jena, Germany, in January 2009. The CRDS analyzer response was very linear, with residual errors for CO<sub>2</sub> below 0.02 ppm for the range from 354.71 ppm to 453.12 ppm and for CH<sub>4</sub> below 0.05 ppb for the range from 1804.73 ppb to 2296.69 ppb.

Both the Harvard and the MPI standard scales are traceable to the WMO CO<sub>2</sub> scales maintained in NOAA/ESRL (Zhao and Tans, 2006). However, there are potential causes for the mean difference of 0.22 ppm (see Table 1) between CO<sub>2</sub> measurements from the NDIR and the CRDS analyzers: 1) CO<sub>2</sub> concentrations of Harvard standards might have drifted due to shipment and one year's storage; 2) the CRDS analyzer might have drifted since the calibrations were made 4 months before the campaign. For further comparison, we try to place the CRDS and the NDIR on the same calibration scale. To perform this, we use the measurements of the four filling tanks by the CRDS analyzer immediately after the last flight of the campaign and assign the CO<sub>2</sub> values derived from the CRDS measurements to the NDIR in-flight calibrations. Since the CRDS analyzer scans the spectrum of the absorption line of <sup>12</sup>C<sup>16</sup>O<sub>2</sub> and uses the peak height obtained from the fit of the spectral line to determine the mixing ratio of total CO<sub>2</sub> in air, the measurements are sensitive to variations of compositions (N<sub>2</sub>, O<sub>2</sub>, and Ar) due to pressure broadening and to variations of carbon isotopologues. Therefore, the measurements of the four standard gases need to be corrected for the pressure-broadening and isotope effects.

Title Page

Abstract

Introduction

Conclusions

References

Tables

Figures

⏪

⏩

◀

▶

Back

Close

Full Screen / Esc

Printer-friendly Version

Interactive Discussion

[Title Page](#)[Abstract](#)[Introduction](#)[Conclusions](#)[References](#)[Tables](#)[Figures](#)[⏪](#)[⏩](#)[◀](#)[▶](#)[Back](#)[Close](#)[Full Screen / Esc](#)[Printer-friendly Version](#)[Interactive Discussion](#)

Unfortunately, the inert background gas fractions ( $N_2$ ,  $O_2$ , and Ar) of the four filling tanks have not been measured. However, the Lorentzian broadening parameter was measured as part of the field campaign, and that data, along with a laboratory investigation of the dependence of the peak height of the absorption lines on Lorentzian broadening, were used to correct the calibration tank data reported by the CRDS analyzer.

## 6.1 Corrections for the pressure-broadening effect

The high-resolution spectral profile of  $^{12}C^{16}O_2$  was recorded and was fitted using a Galatry profile model (Varghese and Hanson, 1984). In the Galatry model, pressure broadening consists of Lorentzian broadening (parameterized as the variable  $y$ , line width) and line narrowing (parameterized as the variable  $z$ ). Both  $y$  and  $z$  vary according to the variations of compositions in air. Ideally, changes in both  $y$  and  $z$  should be used to correct the pressure-broadening effect for measurements of synthetic air. However, the  $z$  parameter was not independently fitted during those measurements in Brazil. Therefore, we only discuss correcting the pressure-broadening effect based on the variation in the  $y$  parameter, assuming that the  $z$  parameter is linearly correlated to the  $y$  parameter. For constant mixing ratios of  $CO_2$  in air, the Galatry profiles vary according to  $y$ , while the areas of the profiles are constant (see Fig. 4a). The correlation between the normalized peak height and the width of the spectral profiles is shown in Fig. 4b. Theoretical calculation predicts the following equation:

$$\frac{d[\text{peak}]}{dy} = B \times y + A \quad (1)$$

Here  $[\text{peak}] = \Delta\text{peak}/\text{peak}$ . For measurements of synthetic air standards, the  $y$  varies in such a very small range that  $\frac{d[\text{peak}]}{dy}$  can be regarded as a constant. This constant value was determined from a laboratory experiment of measuring three synthetic air standards by a CRDS analyzer and a GC (Gas Chromatography) to be  $0.34 \pm 0.03$ .

Based on this correlation, we can correct the measured peak height using the  $y$  parameters to compensate the pressure-broadening effect due to variations of compositions in air.

The corrections for the pressure-broadening effect ranged from  $-0.22$  ppm to  $1.68$  ppm for the four filling tanks. The uncertainty of this correction is mainly caused by the noise in the  $y$  parameter due to imperfect mathematical fit. For 5-min measurements of the filling tanks, the error of the mean of the pressure-broadening corrections is estimated to be  $0.11$  ppm.

## 6.2 Corrections for variations in carbon isotopologues

The CRDS analyzer measures the number of  $^{12}\text{C}^{16}\text{O}_2$  molecules, and determines total  $\text{CO}_2$  by dividing the fractional abundance of  $^{12}\text{C}^{16}\text{O}_2$  in ambient air according to the calibration of the CRDS analyzer in the laboratory. The fractional abundance of synthetic air can be different from that of ambient air since the  $\text{CO}_2$  in the synthetic air was from burned petroleum or natural gases. The isotopologues that could affect the measurements of total  $\text{CO}_2$  by more than  $0.01$  ppm are  $^{13}\text{C}^{16}\text{O}_2$  and  $^{12}\text{C}^{16}\text{O}^{18}\text{O}$  (Tohjima et al., 2009).

Practically, their fractional abundance can be derived from measurements of  $^{13}\text{C}/^{12}\text{C}$  and  $^{18}\text{O}/^{16}\text{O}$  isotopic ratios. In the following, we will discuss the impacts of variations in the two isotopologues on the CRDS  $\text{CO}_2$  measurements. The  $^{13}\text{C}/^{12}\text{C}$  isotopic ratios are normally expressed as  $\delta^{13}\text{C}$  values and are defined as follows:

$$\delta^{13}\text{C}(\text{‰}) = \left[ \frac{^{13}\text{R}_{\text{sample}}}{^{13}\text{R}_{\text{reference}}} - 1 \right] \times 10^3 \quad (2)$$

Here  $^{13}\text{R}_{\text{sample}} = ^{13}\text{C}/^{12}\text{C}_{\text{sample}}$ ,  $^{13}\text{R}_{\text{reference}} = ^{13}\text{C}/^{12}\text{C}_{\text{reference}}$ . The  $\delta^{13}\text{C}$  values are expressed relative to the absolute  $^{13}\text{C}/^{12}\text{C}$  ratio of  $0.011180 \pm 0.000028$  for the reference materials of the Vienna Pee Dee Belemnite (VPDB) (Tohjima et al., 2009).

Title Page

Abstract

Introduction

Conclusions

References

Tables

Figures

◀

▶

◀

▶

Back

Close

Full Screen / Esc

Printer-friendly Version

Interactive Discussion

Similarly, the  $^{18}\text{O}/^{16}\text{O}$  isotopic ratios are expressed as  $\delta^{18}\text{O}$  values and are defined as

$$\delta^{18}\text{O}(0/00) = \left[ \frac{^{18}\text{R}_{\text{sample}}}{^{18}\text{R}_{\text{reference}}} - 1 \right] \times 10^3 \quad (3)$$

Here  $^{18}\text{R}_{\text{sample}} = ^{18}\text{O}/^{16}\text{O}_{\text{sample}}$ ,  $^{18}\text{R}_{\text{reference}} = ^{18}\text{O}/^{16}\text{O}_{\text{reference}}$ . The  $\delta^{18}\text{O}$  values are expressed relative to the ratio of Vienna Standard Mean Ocean Water (VSMOW), an isotopic water standard. The  $^{18}\text{O}/^{16}\text{O}$  ratio of the VSMOW is  $2.00520 \times 10^{-3}$  (Baertschi, 1976). When measuring synthetic air, the CRDS analyzer calculated the  $\text{CO}_2$  mixing ratio by using the  $^{13}\text{C}/^{12}\text{C}$  and  $^{18}\text{O}/^{16}\text{O}$  ratios of ambient air. The readings of synthetic  $\text{CO}_2$  measurements can be expressed as:

$$\text{CO}_{2\text{meas}} = ^{12}\text{C}^{16}\text{O}_2 \times (1 + ^{13}\text{R}_{\text{amb}} + 2 \times ^{18}\text{R}_{\text{amb}}) \quad (4)$$

However, the  $\text{CO}_2$  mixing ratio of the synthetic air should be calculated as:

$$\text{CO}_{2\text{syn}} = ^{12}\text{C}^{16}\text{O}_2 \times (1 + ^{13}\text{R}_{\text{syn}} + 2 \times ^{18}\text{R}_{\text{syn}}) \quad (5)$$

Here,  $\text{CO}_2$  and  $^{12}\text{C}^{16}\text{O}_2$  denote the total  $\text{CO}_2$  mixing ratio and the mixing ratio of  $^{12}\text{C}^{16}\text{O}_2$ , respectively. From Eqs. (2)–(5), we can derive the equation for calculating  $\text{CO}_2$  in the synthetic air

$$\text{CO}_{2\text{syn}} = \text{CO}_{2\text{meas}} \times \left[ \frac{1 + ^{13}\text{R}_{\text{ref}} \times (1 + \delta^{13}\text{C}_{\text{syn}}) + 2 \times ^{18}\text{R}_{\text{ref}} \times (1 + \delta^{18}\text{C}_{\text{syn}})}{1 + ^{13}\text{R}_{\text{ref}} \times (1 + \delta^{13}\text{C}_{\text{amb}}) + 2 \times ^{18}\text{R}_{\text{ref}} \times (1 + \delta^{18}\text{C}_{\text{amb}})} \right] \quad (6)$$

The  $\delta^{13}\text{C}$  and  $\delta^{18}\text{O}$  values of ambient  $\text{CO}_2$  are around  $-8\text{‰}$  on the VPDB scale (GLOBALVIEW-CO2C13) and around  $42\text{‰}$  on the VSMOW scale (Allison and Francey, 2007), respectively. Unfortunately, direct  $\delta^{13}\text{C}$  and  $\delta^{18}\text{O}$  measurements for the four filling tanks are not available and not easy to obtain due to logistic difficulties. A good estimate for the  $\delta^{13}\text{C}$  and  $\delta^{18}\text{O}$  values of the four filling tanks is  $-37 \pm 11\text{‰}$  on the

Title Page

Abstract

Introduction

Conclusions

References

Tables

Figures

⏪

⏩

◀

▶

Back

Close

Full Screen / Esc

Printer-friendly Version

Interactive Discussion



VPDB scale and  $24 \pm 10\%$  on the VSMOW scale, respectively. The corrections due to variations of  $\delta^{13}\text{C}$  and  $\delta^{18}\text{O}$  values for the filling tanks using these values are  $0.14 \sim 0.16 \pm 0.06$  ppm, which are small corrections compared to the corrections for the above pressure-broadening effect.

After the above described corrections, the total  $\text{CO}_2$  values of the filling tanks were finally determined (see Table 2). However, the assigned values to the NDIR in-flight calibrations need to incorporate the isotope effect for the original calibrations as well since they were performed against ambient air standards by an NDIR analyzer (modified Li-Cor, Inc. LI-6251). The isotope effect of an NDIR analyzer can be evaluated based on the relative molar response (RMR) value of the NDIR analyzer and the difference in the mole fraction of the isotopologues between the ambient and the synthetic air (Tohjima et al., 2009). We employed the RMR values obtained by Tohjima et al. (2009) and the mole fraction differences described above to estimate the isotope effect and found out the original calibrations were  $0.09 \pm 0.02$  ppm higher than corresponding total  $\text{CO}_2$  mixing ratios. Notice that no correction was required when the NDIR analyzer was used to measure atmospheric air since the isotope effect was cancelled out. Therefore, the assigned value to the NDIR in-flight calibrations should be the determined total  $\text{CO}_2$  values by the CRDS plus 0.09 ppm (see Table 2).

The differences between the values assigned to the NDIR and the Harvard calibration values are listed as well. The values assigned for the four tanks were applied as the standards to reprocess the NDIR data. The comparisons between the CRDS and the reprocessed NDIR data are shown in Table 1. The mean difference between the two analyzers is reduced to  $0.05 \pm 0.09$  ppm. The uncertainties related to the comparison between the two  $\text{CO}_2$  analyzers are summed up in Table 3. The total uncertainty related to the comparison is estimated to be 0.14 ppm. The high agreement between the measurements of the CRDS and the NDIR analyzers after placing them on the same scale proved that 1) the CRDS analyzer during the BARCA phase B campaign was highly stable ( $\sim 0.05$  ppm); 2) water corrections for  $\text{CO}_2$  and  $\text{CH}_4$  using simultaneously measured water vapor were fully adequate.

---

**High-accuracy  
continuous airborne  
measurements of  
greenhouse gases**H. Chen et al.

---

[Title Page](#)[Abstract](#)[Introduction](#)[Conclusions](#)[References](#)[Tables](#)[Figures](#)[⏪](#)[⏩](#)[◀](#)[▶](#)[Back](#)[Close](#)[Full Screen / Esc](#)[Printer-friendly Version](#)[Interactive Discussion](#)

The accuracy of the CO<sub>2</sub> measurements of the CRDS analyzer during BARCA relative to the WMO scale is dependent on potential drift of the analyzer; the accuracy will be better than 0.05 ppm when the CRDS analyzer is recalibrated by ambient air standards to remove potential drift over a long term operation.

## 7 Conclusions

High-accuracy continuous measurements of greenhouse gases during the BARCA phase B campaign were achieved by an analyzer based on the cavity ring-down spectroscopy technique. Water correction functions derived from the laboratory experiments were used to correct the dilution and pressure-broadening effects due to variations of water vapor mixing ratios. The water correction functions have been shown to be transferable between different analyzers of the same type. The CRDS analyzer performed highly stably under simulated flight conditions of varying environmental pressure and temperature in an environmental chamber. The comparison of CO<sub>2</sub> measurements made by the CRDS analyzer and an NDIR analyzer on board the same aircraft showed a mean difference of  $0.22 \pm 0.09$  ppm, and a mean standard deviation of  $0.23 \pm 0.05$  ppm for all flights over the Amazon rain forest. Measurements of synthetic air from the filling tanks of the NDIR analyzer at the end of the campaign were carried out and the concentrations were determined after correcting for the variation in carbon isotopologues and for pressure-broadening effects due to variations of compositions in synthetic air. Application of these cross-calibrations reduced the mean of the difference between the CRDS and the NDIR during the campaign to  $0.05 \pm 0.09$  ppm. The CRDS analyzer performed highly stably without drying the sample air and without in-flight calibrations during the BARCA campaign phase B. The results clearly show that a single set of calibrations of the CRDS analyzer using ambient air standards during the aircraft campaign guarantees accuracy better than 0.05 ppm.

### High-accuracy continuous airborne measurements of greenhouse gases

H. Chen et al.

Title Page

Abstract

Introduction

Conclusions

References

Tables

Figures

⏪

⏩

◀

▶

Back

Close

Full Screen / Esc

Printer-friendly Version

Interactive Discussion



*Acknowledgements.* We are grateful for the efforts of the pilots P. Celso and D. Gramacho and the other BARCA team members P. Artaxo, F. Morais, A. C. Ribeiro, K. M. Longo, K. Wiedemann, M. D. P. Longo, M. A. F. de Silva Dias, L. Gatti, M. O. Andreae and N. Juergens. We are thankful for the discussions and information sharing with C. Sweeney and A. Karion.

5 We also thank A. Jordan for discussions about standard gases and W. A. Brand for discussions about carbon isotopes. Funding for the BARCA flights was provided by Max Planck Society, NASA and Millennium Institute of the Large Scale Biosphere – Atmosphere Experiment in Amazonia (LBA).

10 The service charges for this open access publication have been covered by the Max Planck Society.

## References

- Allison, C. E. and Francey, R. J.: Verifying Southern Hemisphere trends in atmospheric carbon dioxide stable isotopes, *J. Geophys. Res.-Atmos.*, 112, 112, D21304, doi:10.1029/2006JD007345, 2007 2007.
- 15 Anderson, B. E., Gregory, G. L., Collins, J. E., Sachse, G. W., Conway, T. J., and Whiting, G. P.: Airborne observations of spatial and temporal variability of tropospheric carbon dioxide, *J. Geophys. Res.-Atmos.*, 101, 1985–1997, 1996.
- Baertschi, P.: Absolute O–18 content of standard mean ocean water, *Earth Planet. Sc. Lett.*, 20 31, 341–344, 1976.
- Bischof, W.: Variations in concentration of carbon dioxide in the free atmosphere, *Tellus*, 14, 87–90, 1962.
- Boering, K. A., Daube, B. C., Wofsy, S. C., Loewenstein, M., Podolske, J. R., and Keim, E. R.: Tracer-tracer relationships and lower stratospheric dynamics – CO<sub>2</sub> and N<sub>2</sub>O correlations during spade, *Geophys. Res. Lett.*, 21, 2567–2570, 1994.
- 25 Crosson, E. R.: A cavity ring-down analyzer for measuring atmospheric levels of methane, carbon dioxide, and water vapor, *Appl. Phys. B-Lasers O.*, 92, 403–408, 2008.
- Daube, B. C., Boering, K. A., Andrews, A. E., and Wofsy, S. C.: A high-precision fast-response airborne CO<sub>2</sub> analyzer for in situ sampling from the surface to the middle stratosphere, *J. Atmos. Ocean. Tech.*, 19, 1532–1543, 2002.
- 30

## High-accuracy continuous airborne measurements of greenhouse gases

H. Chen et al.

Title Page

Abstract

Introduction

Conclusions

References

Tables

Figures

◀

▶

◀

▶

Back

Close

Full Screen / Esc

Printer-friendly Version

Interactive Discussion

**High-accuracy  
continuous airborne  
measurements of  
greenhouse gases**

H. Chen et al.

Title Page

Abstract

Introduction

Conclusions

References

Tables

Figures

◀

▶

◀

▶

Back

Close

Full Screen / Esc

Printer-friendly Version

Interactive Discussion

- Frankenberg, C., Bergamaschi, P., Butz, A., Houweling, S., Meirink, J. F., Notholt, J., Petersen, A. K., Schrijver, H., Warneke, T., and Aben, I.: Tropical methane emissions: a revised view from SCIAMACHY onboard ENVISAT, *Geophys. Res. Lett.*, 35, L15811, doi:10.1029/2008GL034300, 2008.
- 5 Heimann, M.: Searching out the sinks, *Nat. Geosci.*, 2, 3–4, 2009.
- Houweling, S., Rockmann, T., Aben, I., Keppler, F., Krol, M., Meirink, J. F., Dlugokencky, E. J., and Frankenberg, C.: Atmospheric constraints on global emissions of methane from plants, *Geophys. Res. Lett.*, 33, L15821, doi:10.1029/2006GL026162, 2006.
- Jimenez, R., Herndon, S., Shorter, J. H., Nelson, D. D., McManus, J. B., and Zahniser, M. S.:  
10 Atmospheric trace gas measurements using a dual quantum-cascade laser n-dd-infrared absorption spectrometer, *P. Soc. Photo.-Opt. Ins.*, 5738, 318–331, 2005.
- Keeling, C. D., Harris, T. B., and Wilkins, E. M.: Concentration of atmospheric carbon dioxide at 500 and 700 millibars, *J. Geophys. Res.*, 73, 4511–4528, 1968.
- Keppler, F., Hamilton, J. T. G., Brass, M., and Rockmann, T.: Methane emissions from terrestrial plants under aerobic conditions, *Nature*, 439, 187–191, 2006.
- 15 Levin, I., Ciais, P., Langenfelds, R., Schmidt, M., Ramonet, M., Sidorov, K., Tchebakova, N., Gloor, M., Heimann, M., Schulze, E. D., Vygodskaya, N. N., Shibistova, O., and Lloyd, J.: Three years of trace gas observations over the EuroSiberian domain derived from aircraft sampling – a concerted action, *Tellus B*, 54, 696–712, 2002.
- 20 Machida, T., Kita, K., Kondo, Y., Blake, D., Kawakami, S., Inoue, G., and Ogawa, T.: Vertical and meridional distributions of the atmospheric CO<sub>2</sub> mixing ratio between northern midlatitudes and southern subtropics, *J. Geophys. Res.-Atmos.*, 108, 108(D3), 8401, doi:10.1029/2001JD000910, 2002.
- Machida, T., Matsueda, H., Sawa, Y., Nakagawa, Y., Hirotani, K., Kondo, N., Goto, K.,  
25 Nakazawa, T., Ishikawa, K., and Ogawa, T.: Worldwide measurements of atmospheric CO<sub>2</sub> and other trace gas species using commercial airlines, *J. Atmos. Ocean. Tech.*, 25, 1744–1754, 2008.
- Miller, J. B., Gatti, L. V., d’Amelio, M. T. S., Crotwell, A. M., Dlugokencky, E. J., Bakwin, P., Artaxo, P., and Tans, P. P.: Airborne measurements indicate large methane emissions from the eastern Amazon basin, *Geophys. Res. Lett.*, 34, L10809, doi:10.1029/2006GL029213,  
30 2007.
- Richardson, S. J., Miles, N. L., Davis, K. J., and Crosson, E. R.: Filed testing and error analysis of cavity ringdown spectroscopy instruments measuring CO<sub>2</sub>, 15th WMO/IAEA meeting of

experts on carbon dioxide, other greenhouse gases, and related tracer measurement techniques, 7–10 September 2009, Jena, Germany, 2009.

Shashkov, A., Higuchi, K., and Chan, D.: Aircraft vertical profiling of variation of CO<sub>2</sub> over a Canadian boreal forest site: a role of advection in the changes in the atmospheric boundary layer CO<sub>2</sub> content, *Tellus B*, 59, 234–243, 2007.

Tans, P. P., Bakwin, P. S., and Guenther, D. W.: A feasible global carbon cycle observing system: a plan to decipher today's carbon cycle based on observations, *Glob. Change Biol.*, 2, 309–318, 1996.

Tohjima, Y., Katsumata, K., Morino, I., Mukai, H., Machida, T., Akama, I., Amari, T., and Tsunogai, U.: Theoretical and experimental evaluation of the isotope effect of NDIR analyzer on atmospheric CO<sub>2</sub> measurement, *J. Geophys. Res.-Atmos.*, 114, D13302, doi:10.1029/2009JD011734, 2009.

Varghese, P. L. and Hanson, R. K.: Collisional narrowing effects on spectral-line shapes measured at high-resolution, *Appl. Optics*, 23, 2376–2385, 1984.

WMO (2003) Report of the 11th WMO/IAEA Meeting of Experts on Carbon Dioxide Concentration and Related Tracer Measurement Techniques, Tokyo, Japan, 25–28 September 2001, Tech. Rep. 148, World Meteorological Organisation – Global Atmospheric Watch, Geneva, Switzerland.

Zhao, C. L. and Tans, P. P.: Estimating uncertainty of the WMO mole fraction scale for carbon dioxide in air, *J. Geophys. Res.-Atmos.*, 111, D08S09, doi:10.1029/2005JD006003, 2006.

## High-accuracy continuous airborne measurements of greenhouse gases

H. Chen et al.

Title Page

Abstract

Introduction

Conclusions

References

Tables

Figures

◀

▶

◀

▶

Back

Close

Full Screen / Esc

Printer-friendly Version

Interactive Discussion

**Table 1.** Comparisons of the CRDS with an NDIR analyzer.

| Flight No.                                      | Date (mmdd) | Difference (ppm) | Difference $1\sigma$ (ppm) | Difference after cross-calibration (ppm) | Difference after cross-calibration $1\sigma$ (ppm) |
|---|-------------|------------------|----------------------------|--|--|
| 000   | 0511        | 1.39             | 0.87                       | –  | –  |
| 001   | 0515        | 0.28             | 0.20                       | –  | –  |
| 002   | 0517        | 0.20             | 0.23                       | 0.06                                     | 0.25   |
| 003   | 0517        | 0.22             | 0.20                       | 0.06                                     | 0.20   |
| 004   | 0519        | 0.34             | 0.32                       | 0.19                                     | 0.32   |
| 005   | 0519        | 0.21             | 0.28                       | 0.03                                     | 0.26   |
| 006   | 0521        | 0.12             | 0.22                       | -0.04                                    | 0.22   |
| 007   | 0521        | 0.11             | 0.26                       | -0.05                                    | 0.25   |
| 008   | 0522        | –                | –                          | –  | –  |
| 009   | 0523        | –                | –                          | –  | –  |
| 010   | 0523        | –                | –                          | –  | –  |
| 011   | 0526        | 0.20             | 0.18                       | 0.03                                     | 0.19   |
| 012   | 0526        | 0.18             | 0.15                       | 0.01                                     | 0.16   |
| 013   | 0527        | 0.38             | 0.23                       | 0.22                                     | 0.23   |
| 014   | 0527        | –                | –                          | –  | –  |
| 015   | 0528        | 0.21             | 0.22                       | 0.03                                     | 0.22   |
| Average (not including flight Nos. 000 and 001) |             | 0.22             | 0.23                       | 0.05                                     | 0.23   |

## High-accuracy continuous airborne measurements of greenhouse gases

H. Chen et al.

Title Page

Abstract

Introduction

Conclusions

References

Tables

Figures

◀

▶

◀

▶

Back

Close

Full Screen / Esc

Printer-friendly Version

Interactive Discussion

## High-accuracy continuous airborne measurements of greenhouse gases

H. Chen et al.

**Table 2.** Cross-calibration.

| Tanks     | Total CO <sub>2</sub> values<br>derived from<br>the CRDS<br>measurements<br>(ppm) | Assigned to<br>the NDIR<br>(ppm) | Harvard<br>calibrations<br>(ppm) | Difference between<br>the assigned<br>Harvard (ppm) |
|-----------|---|----------------------------------|----------------------------------|---|
| Low span  | 362.70  | 362.79                           | 362.87                           | −0.08   |
| Target    | 371.72  | 371.81                           | 371.61                           | 0.20  |
| Reference | 383.40  | 383.49                           | 383.30*                          | 0.19  |
| High span | 405.10  | 405.19                           | 405.41                           | −0.22   |

\* not directly calibrated, but derived from the target calibration gas (due to logistic difficulties)

[Title Page](#)
[Abstract](#)
[Introduction](#)
[Conclusions](#)
[References](#)
[Tables](#)
[Figures](#)
[Back](#)
[Close](#)
[Full Screen / Esc](#)
[Printer-friendly Version](#)
[Interactive Discussion](#)

## High-accuracy continuous airborne measurements of greenhouse gases

H. Chen et al.

**Table 3.** Uncertainties related to comparison between the two CO<sub>2</sub> analyzers.

| Sources  | Uncertainties<br>(ppm) | Remarks  |
|--|------------------------|--|
| Water correction                               | 0.05                   | Maximum residual error   |
| Corrections for<br>pressure broadening         | 0.11                   | The error of the mean of corrections<br>for pressure broadening                      |
| Carbon isotope correction                      | 0.06                   | Uncertainties in estimated $\delta^{13}\text{C}$<br>and $\delta^{18}\text{O}$ values |
| Carbon isotope effects<br>on the NDIR analyzer | 0.02                   | Variations of RMRs for different<br>NDIR analyzers                                   |
| Total uncertainty                              | 0.14                   |  |

[Title Page](#)
[Abstract](#)
[Introduction](#)
[Conclusions](#)
[References](#)
[Tables](#)
[Figures](#)
[I◀](#)
[▶I](#)
[◀](#)
[▶](#)
[Back](#)
[Close](#)
[Full Screen / Esc](#)
[Printer-friendly Version](#)
[Interactive Discussion](#)

**High-accuracy  
continuous airborne  
measurements of  
greenhouse gases**

H. Chen et al.

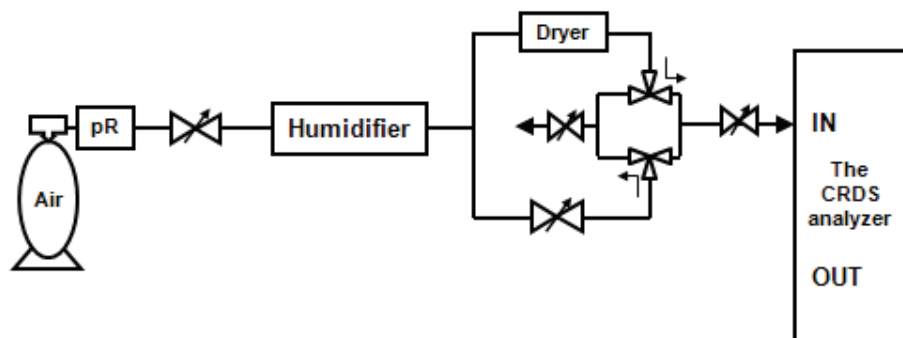


**Fig. 1.** Schematic of the setup for experiments to derive water vapor correction functions.

[Title Page](#)[Abstract](#)[Introduction](#)[Conclusions](#)[References](#)[Tables](#)[Figures](#)[◀](#)[▶](#)[◀](#)[▶](#)[Back](#)[Close](#)[Full Screen / Esc](#)[Printer-friendly Version](#)[Interactive Discussion](#)

## High-accuracy continuous airborne measurements of greenhouse gases

H. Chen et al.

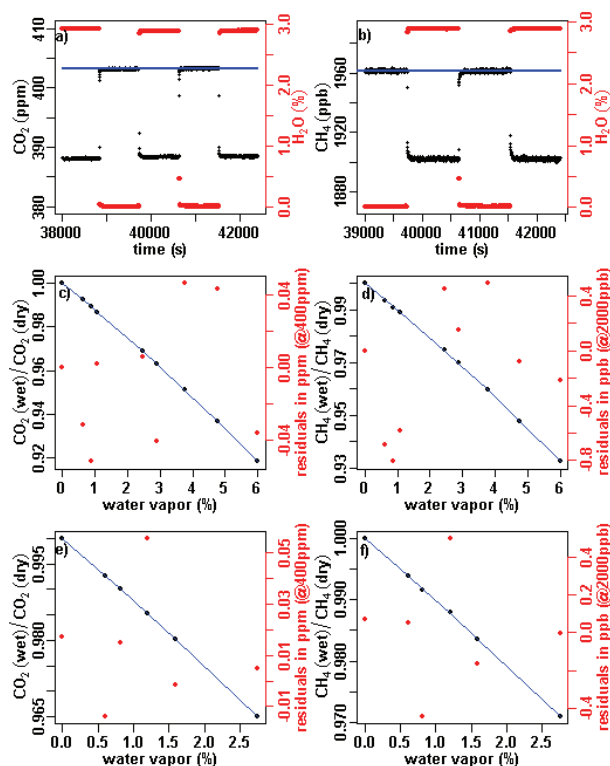


**Fig. 2.** (a, b) Examples of the responses of CO<sub>2</sub> and CH<sub>4</sub> while switching between wet and dry air (see H<sub>2</sub>O on the right axis), and linear drift corrections (blue lines). (c, d) Quadratic fits of CO<sub>2</sub>wet/CO<sub>2</sub>dry and CH<sub>4</sub>wet/CH<sub>4</sub>dry vs. H<sub>2</sub>O mixing ratios. (e, f) Results from similar experiments performed with CFADS15, with the curve showing the fit from experiments using CFADS37. The red dots in (a–d) are residuals of corresponding fits and are read on the axis to the right. Note that (a–d) are results from experiments performed with CFADS37 and (e, f) with CFADS15.

Title Page

Abstract

Introduction

Conclusions

References

Tables

Figures

◀

▶

◀

▶

Back

Close

Full Screen / Esc

Printer-friendly Version

Interactive Discussion



High-accuracy  
continuous airborne  
measurements of  
greenhouse gases

H. Chen et al.

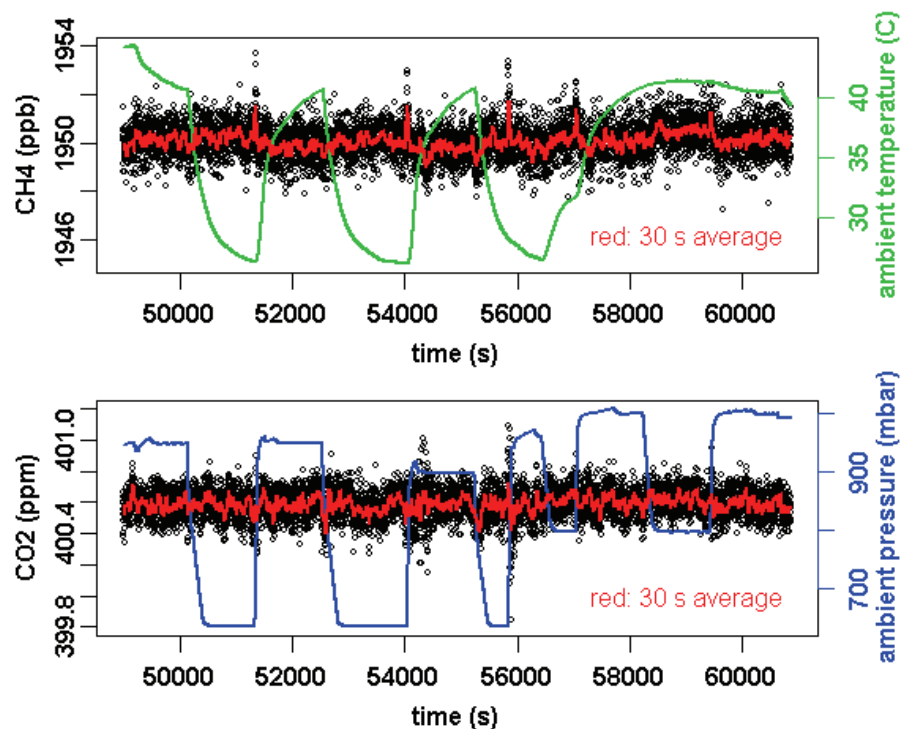


**Fig. 3.** CO<sub>2</sub> and CH<sub>4</sub> measurements under simulated flight conditions. Variations of temperature and pressure are shown on the axis to the right.

[Title Page](#)[Abstract](#)[Introduction](#)[Conclusions](#)[References](#)[Tables](#)[Figures](#)[◀](#)[▶](#)[◀](#)[▶](#)[Back](#)[Close](#)[Full Screen / Esc](#)[Printer-friendly Version](#)[Interactive Discussion](#)

High-accuracy  
continuous airborne  
measurements of  
greenhouse gases

H. Chen et al.

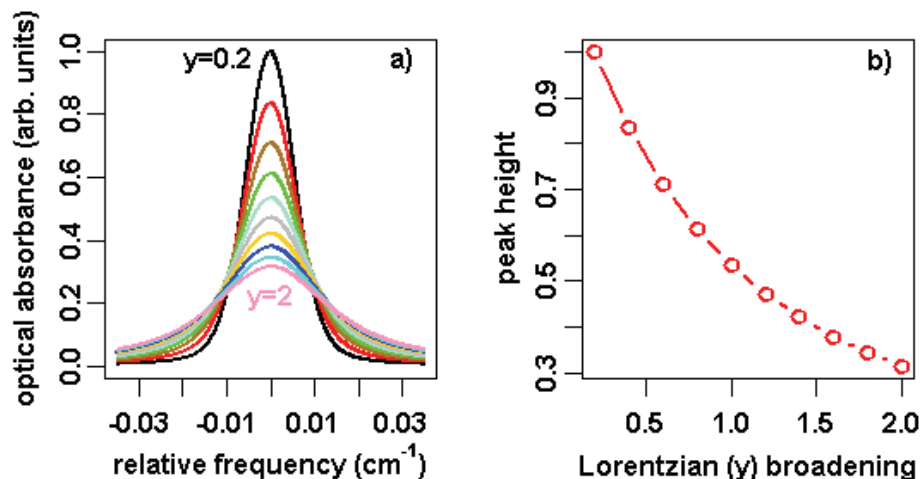


**Fig. 4.** (a) normalized absorption profiles for constant concentrations; (b) correlation between peak height and Lorentzian ( $y$ ) broadening.

[Title Page](#)[Abstract](#)[Introduction](#)[Conclusions](#)[References](#)[Tables](#)[Figures](#)[◀](#)[▶](#)[◀](#)[▶](#)[Back](#)[Close](#)[Full Screen / Esc](#)[Printer-friendly Version](#)[Interactive Discussion](#)